MDPI

Effects of Recycled Sponge Iron on Phosphorus Recovery from Polluted Water

Ping Cheng [1], Biao Wang [1],*, Xiaohuan Wang [2] and Wei Xiao [1]

[1] School of Resources Engineering, Xi'an University of Architecture and Technology, Xi'an 710055, China; chengp_314@163.com (P.C.); wei.xiao@xauat.edu.cn (W.X.)
[2] School of Economics and Technology, Anhui Agricultural University, Hefei 230036, China; wxh17733351152@163.com
* Correspondence: wb1056669818@163.com; Tel.: +86-029-8220-3408

Abstract: Phosphorus in water not only degrades water quality but also leads to a waste of resources. In this study, adsorption thermodynamics and kinetics were used to study the effect of sponge iron on phosphorus removal, and a filtration bed was used to simulate the phosphorus removal in polluted water. The results showed that the maximum theoretical adsorption capacity of the modified sponge iron was increased from 4.17 mg/g to 18.18 mg/g. After desorption with 18.18 mol/L of sodium hydroxide and reactivation with 6% (w%) sulfuric acid, the activation rate of modified sponge iron can reach 98%. In a continuous operation experiment run for approximately 200 days, the sponge iron phosphorus removal percolation bed showed a good phosphorus removal ability. Under the condition of TP = 10 mg/L, HRT = 1 H, the comprehensive phosphorus removal rate was 30–89%, and the accumulated phosphorus adsorption per unit volume was 6.95 kg/m^3. Wastewater from the regeneration of the sponge iron base can be used to recover guano stone. The optimum conditions were pH = 10, n (Mg^{2+}):n (PO$_4^{3-}$):n (NH^{4+}) = 1.3:1:1.1. Under the optimum conditions, the phosphorus recovery rate could reach 97.8%. The method provided in this study has theoretical and practical significance for the removal and recycling of phosphorus in polluted water.

1. Introduction

With the rapid development of industry and agriculture, China's phosphorus emissions have increased dramatically, which has led to high phosphorus content in water [1,2]. Phosphorus is one of the most important factors causing the eutrophication of water [3]. When the concentration of phosphorus in water is more than 0.3 mg/L, it can easily cause algae and aquatic plants to propagate in large quantities [4]. On the other hand, phosphorus in nature is also a non-renewable resource. Unlike petrochemical resources, no substance can fill the role of phosphorus in industrial and agricultural production in the world [5–7]. At present, wastewater treatment in the field of environmental protection in China relies mainly on dephosphorization, and there are still serious deficiencies in phosphorus recovery and utilization [8,9].

An increasing number of researchers are interested in the recovery of phosphate from water. Various technologies have been used to effectively restore water quality containing phosphate, such as reverse osmosis [10], sedimentation [11], biological processes [12], constructed wetland [13], ion exchange [14], membrane [15], electrochemistry [16], adsorption [17,18] and flotation [19]. Other methods have many limitations, such as complex operation and the use of a large number of chemical reagents; in addition, the sludge produced is difficult to treat, and regeneration is difficult and unstable [20,21]. Among these methods, the adsorption method is widely used in phosphate removal because of its simple operating conditions, high cost-effectiveness, eco-friendliness, large adsorption capacity and low sludge production [22].

Thus far, researchers have introduced several adsorbents with high porosity to effectively adsorb phosphate in sewage. These adsorbents, such as organic polymers [23,24], mesoporous silica [25], activated carbon [26], red mud [20,27] and zeolite [28], have a high specific surface area. One of the main disadvantages of these adsorbents is that they are usually difficult to separate and recover from the water medium, which requires additional separation technology [29,30].

Fe-based technologies have been extensively investigated for phosphate removal from the wastewater [31,32]. The zero-valent iron (ZVI)/sand bed reactor reported by Sleiman et al. achieved maximum removal capacity of 132 mg P/g Fe [33]. Sponge iron is a new type of zero-valent iron material, which has the advantages of low carbon porosity, large specific surface area, low price, low hardenability, high active iron content, and strong electrochemical enrichment, physical adsorption and flocculation sedimentation characteristics [32,34]. Today, smelting sponge iron in induction furnaces is one of the main processes in steel production. In this process, raw materials (sponge iron and scrap) are melted by inducing electromagnetic currents. Sponge iron has small cavities and is porous [18]. At present, sponge iron is mostly used for the deoxidization of industrial water, and it has been shown that it has good adsorption and phosphorus removal characteristics [35–38]. However, research on the removal and recovery of phosphorus products based on a sponge iron percolation bed has not been carried out.

Sponge iron is currently mostly used for the deoxygenation of industrial water. Studies have shown that sponge iron has good adsorption and dephosphorization characteristics [35]. However, sponge iron is modified to improve its phosphorus adsorption performance, and a percolation bed based on sponge iron is constructed to remove and recover phosphorus products [2,6].

Therefore, this paper studies the sponge iron modification method and discusses the adsorption kinetic characteristics of sponge iron before and after modification, investigates the dynamic phosphorus removal characteristics of the percolation bed based on the modified sponge iron, and discusses the reprocessing of sponge iron, the method of living, and the method of preparing struvite by recycling phosphorus resources.

2. Materials and Methods

2.1. Materials and Reagents

The sponge iron used in this experiment was purchased from Gongyi Liansheng Water Treatment Materials Co., Ltd, Zhengzhou, China. The appearance was gray black, the interior was porous and spongy, and the main component was iron. The BET specific surface area of the purchased sponge iron reaches 81 m^2/g. And the zeta potential of sponge iron is 8.03 mV at pH 7.0 [39]. The content of active iron (elemental iron particles with high chemical reaction activity) was more than 90%, the bulk density was 2.2 g/cm^3, and the particle size was 5–8 mm. Ultra-pure water with a conductivity of 18.2 MΩ·cm, used in the experiments, was provided by an USF-ELGA Maxima water purification system (ELGA LabWater, Woodridge, IL, USA). The reagents used in this paper were analytically pure, with certain exceptions.

2.2. Modification of Sponge Iron and Kinetics of Phosphorus Adsorption

The sponge iron was modified by sulfuric acid: we washed the sponge iron with deionized water three times to remove the surface dirt and impurities, and then immersed the sponge iron in 6% sulfuric acid solution in order to modify it for 0.5 h. Finally, we washed it with deionized water to neutrality, and dried it at 105 °C for 1 h.

Static adsorption experiment: we placed 4 g of sponge iron particles before and after modification into a 250 mL conical flask with different concentrations of phosphorus solution of 150 mL, and then placed the conical flask in a constant-temperature shaking bed with a continuous oscillation speed of 150 r/min. The phosphorus content of the solution

was measured at regular intervals. The adsorption amount of phosphorus was calculated by Equation (1), and the adsorption rate curve and adsorption isotherm were drawn.

$$q = V_o \times (C_j - C_e)/m \tag{1}$$

where q is the amount of phosphorus adsorbed by sponge iron (mg/g); m is the quality of sponge ion (g); C_j and C_e are the initial and equilibrium concentrations of phosphorus in the solution, respectively; V_o is the volume of the solution.

2.3. Adsorption Isotherm

The adsorption isotherm shows the strength of the adsorption capacity of the material, and the relationship between the equilibrium concentration and the surface adsorption capacity in the reaction system [1]. The Langmuir adsorption isotherm is based on the two basic assumptions that the adsorbent surface is uniform and there is no interaction between the adsorbate molecules, which are mainly used for the fitting of single molecular layer adsorption. The Freundlich adsorption isotherm is suitable for the fitting of heterogeneous or multi-layer adsorption. The Langmuir equation and Freundlich equation are used to fit and analyze the adsorption isotherms of phosphorus on sponge iron before and after modification. Equation (2) is the Langmuir adsorption isotherm linear form, and Equation (3) is the Freundlich adsorption isotherm linear form:

$$\frac{1}{q_e} = \frac{1}{K_L q_m} \cdot \frac{1}{C_e} + \frac{1}{q_m}, \tag{2}$$

$$\log q_e = \log K_F + \frac{1}{n} \log C_e \tag{3}$$

where q_e is the adsorption amount of phosphorus in adsorption equilibrium (mg/g); C_e is the concentration of phosphorus in adsorption equilibrium (mg/L); q_m is the maximum adsorption amount in theory (mg/g); K_L is the Langmuir adsorption rate constant (L/mg); K_F is the adsorption equilibrium constant; n is the adsorption strength index.

2.4. Desorption and Reactivation of Sponge Iron

We placed 10 g of modified sponge iron into a conical flask containing 100 mL solution with H_3PO_4 1000 mg/L, and it was shaken for 12 h continuously until the adsorption capacity of sponge iron reached saturation. We then measured the phosphorus concentration in the solution, and calculated the phosphorus adsorption capacity (q_{ao}) of the unit weight sponge iron according to Equation (1).

We collected the sponge iron that had reached adsorption saturation, washed it with deionized water three times, added a certain volume of NaOH with the concentration of 1–2 mol/L as a desorption solution and shook it continuously at a constant temperature (25 °C) of 150 r/min for 12 h. We then separated the supernatant, measured the phosphorus concentration (C) in the liquid phase and calculated the desorption amount and desorption rate of the unit modified sponge iron phosphorus; we then reactivated the modified sponge iron with 6% sulfuric acid after desorption, and obtained the regenerated modified sponge iron after drying. Under the same experimental conditions of q_{ao}, the static adsorption test was carried out again to obtain the adsorption amount (q_{a1}) after regeneration of the adsorbent. The calculation methods for the desorption amount (q_d), desorption rate (Z_d) and activation rate (Z_r) of the regenerated adsorbent were as follows:

$$q_d = V \times C/m \tag{4}$$

$$Z_d = q_d/q_{ao} \times 100 \tag{5}$$

$$Z_r = q_{a1}/q_{ao} \times 100 \tag{6}$$

where q_d is the phosphorus desorption of the unit modified sponge iron; Z_d is the desorption efficiency (%); Z_r is the activation efficiency of the regenerated adsorbent (%); V is the volume of desorption solution (L); C is the phosphorus concentration in the alkali regeneration waste liquid (mg/L); m is the mass of adsorption saturated modified sponge iron (g). q_{a0} and q_{a1} are the adsorption amount of phosphorus per unit of modified sponge iron before and after regeneration (mg/g), respectively. Each of the above data are the average of three repeated tests.

2.5. Experiments of Continuous Flow Phosphorus Removal with Sponge Iron

The porous iron filter bed was constructed of 1.7 L organic glass with an inner diameter of 10 cm, height of 100 cm and inner filling height of 60 cm. In order to investigate the removal and enrichment of phosphorus by the percolation bed under the condition of continuous flow, a 10 mg/L concentration of KH_2PO_4 was added to tap water to simulate the phosphorus-bearing water body. During the operation, the hydraulic retention time (HRT) was 1 h, and the temperature was 25 °C. When the phosphorus removal rate tended to be stable, we stopped the operation, used 1 mol/L sodium hydroxide to analyze the sponge iron, and then used 6% sulfuric acid to reactivate the sample and started the next cycle of the dynamic phosphorus removal experiment.

2.6. Recovery of Phosphorus from Waste Liquid of Alkali Regeneration

We transferred the alkali regeneration waste liquid generated in Section 2.3 to a 300 mL beaker and adjusted the regeneration liquid to the expected pH with sulfuric acid; the stirring speed was 150 r/min. We measured the initial phosphorus concentration (C_0) of the alkali regeneration waste liquid, added a certain amount of ammonium salt and magnesium salt in turn 10 min apart, and waited for 30 min after the reaction. The supernatant was filtered by a 0.45 μm membrane, and the phosphorus concentration (C_e) in the filtrate was determined. The phosphorus recovery η was calculated by Equation (7). The precipitates were dried at 40 °C for 48 h and then stored in a desiccator.

$$\eta = (C_0 - C_e)/C_0 \times 100 \tag{7}$$

where, η is the recovery rate of phosphorus; C_0 and C_e are the initial concentration of phosphorus in the alkali regeneration waste liquid and the residual concentration of phosphorus after the formation of struvite, respectively.

2.7. XRD Analysis for Struvite

The XRD of the samples of struvite were analyzed using a D8 Advance X-ray diffractometer (Bruker, Bremen, Germany). The crystal structure parameters of the samples were determined, and the samples were analyzed qualitatively and quantitatively. The ground sample (−0.074 mm) was placed into the groove of the glass sample holder, flattened with ground glass, and inserted into the sample table.

3. Results and Discussion

3.1. Adsorption Kinetics of Phosphorus on the Sponge Iron

3.1.1. Effect of Adsorption Time on Phosphorus Adsorption Capacity

The phosphorus adsorption kinetics of sponge iron before and after modification were compared. The phosphorus adsorption capacity of sponge iron as a function of adsorption time is shown in Figure 1.
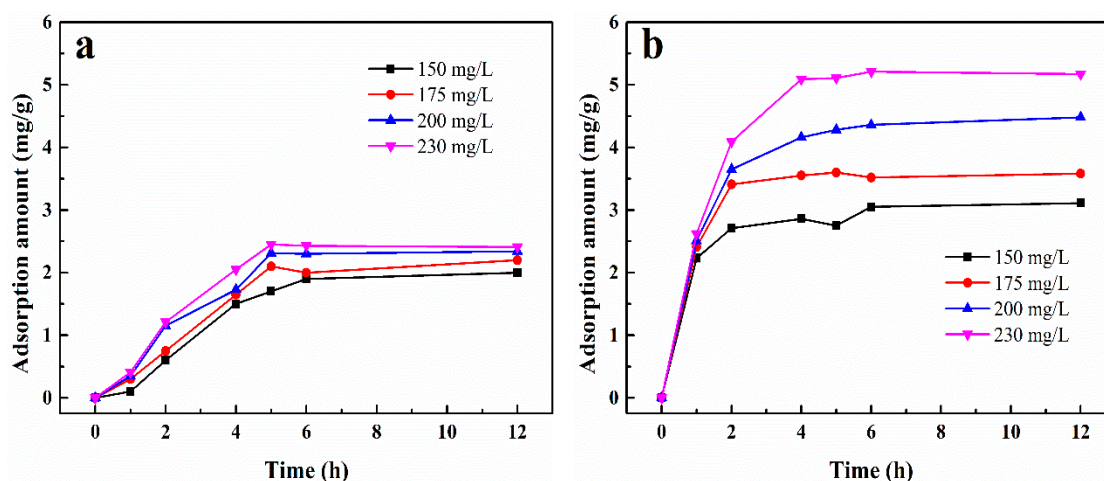
Figure 1. The adsorption amount of phosphorus as a function of adsorption time. ((**a**), unmodified sponge iron; (**b**), modified sponge iron). The initial pH is 7.0 and the concentration of sponge iron is 26.67 mg/mL.

It can be seen that under different initial phosphorus concentrations, the adsorption capacity of sponge iron increases with the increase in adsorption time, and tends to be stable after a period of time. The adsorption equilibrium of unmodified sponge iron was reached after 6 h, while that of modified sponge iron was reduced to 4 h. In the early stage of the adsorption process, the adsorption rate of sponge iron to phosphorus is faster, and the phosphorus removal rate reaches 90% when the adsorption time was 4 h. The reason may be that there are many adsorption points on the surface of sponge iron at the initial stage of adsorption, the difference in ion concentration is large, and phosphorus can be easily combined with the surface of sponge iron [38,40]. With the decrease in adsorption sites on the surface of sponge iron, the adsorption rate slows down and reaches adsorption saturation [35].

3.1.2. Adsorption Isotherm

It can be seen from Figure 2 that the adsorption of phosphorus by sponge iron before and after modification is nonlinear. The fitting coefficients of the Langmuir and Freundlich adsorption isotherms are both greater than 0.95, which can better fit the adsorption process of sponge iron to phosphorus. However, the adsorption behavior is more in line with the Freundlich adsorption isotherm, which indicates that the liquid–solid adsorption reaction is more complex. In the literature of Xiao et. al, the two models are used to study the adsorption of the flotation collector on the mineral surface, and the same conclusion is reached [21]. During the adsorption and modification process, there may be corrosion defects on the surface of the sponge iron and the formation of a heterogeneous surface of iron oxide, and single-layer adsorption and multi-layer adsorption exist at the same time.

It can be seen from the Langmuir adsorption isotherm that the modification of sponge iron can improve the theoretical adsorption capacity of phosphorus. Through sulfuric acid modification, the theoretical adsorption capacity increased from 4.17 mg/g to 18.18 mg/g. The enhancement of the phosphorus adsorption capacity of the modified sponge iron is mainly due to the formation of more iron oxides on the surface of the modified sponge iron; the increase in iron oxides causes the coordination exchange reaction to occur more easily, and there is an increase in active sites on the surface of sponge iron [35,40]. In the Freundlich adsorption isotherm, *n* is related to the difficulty of adsorption, and *n* is more than 1 before and after modification, indicating that the material has better adsorption performance and adsorption is easy.
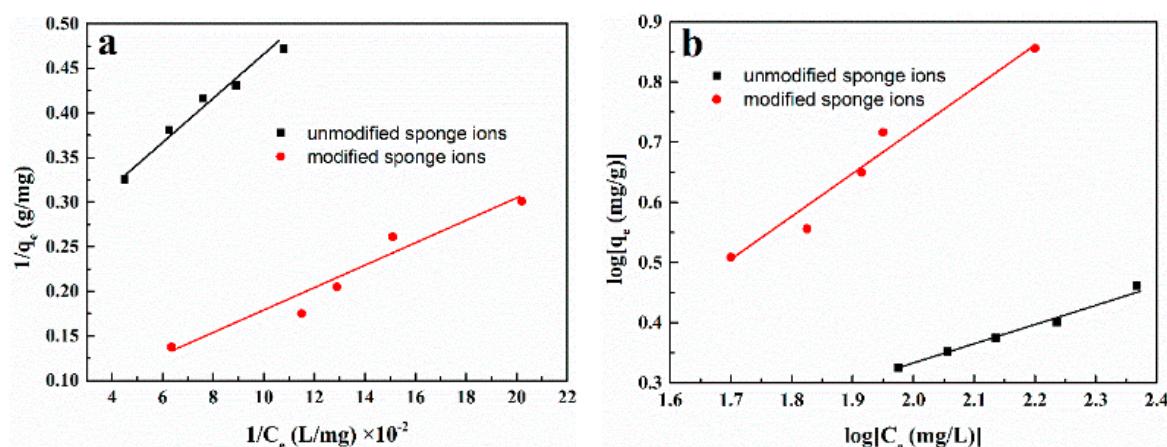
Figure 2. Adsorption isotherm of phosphorus on the sponge iron surface before and after modification. ((**a**), Langmuir isotherm; (**b**), Freundlich isotherm).

3.2. Resorption and Reactivation of Sponge Iron

We took 10 g of saturated modified sponge iron for regeneration, and the regeneration solution was H_2SO_4 solution, HCl solution and NaOH solution, respectively. The influence of the concentration of H_2SO_4 solution, HCl solution and NaOH solution on the desorption rate is shown in Figure 3.
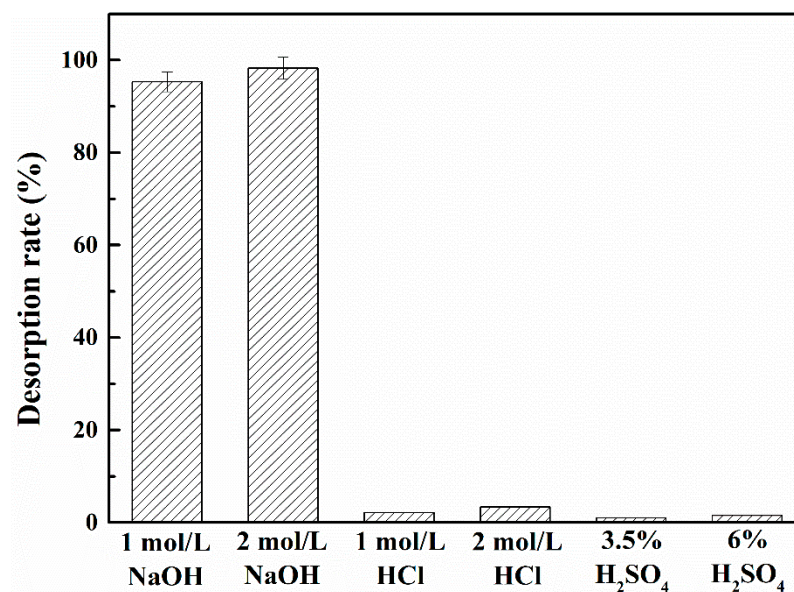

Figure 3. Effect of different solution on desorption of saturated sponge iron.

From the results in Figure 3, it can be seen that H_2SO_4 solution and HCl solution have little desorption capacity for phosphorus; the best desorption effect for phosphorus is NaOH solution of 2 mol/L, but the effect of improving the desorption rate is not obvious compared with that of NaOH solution of 1 mol/L. A balance of efficiency and economy can be achieved by using 1 mol/L NaOH solution as the desorption solution, which is consistent with the reference of Afridi et al. [7].

After phosphorus desorption, it should be reactivated to restore the adsorption performance of the sponge iron. The reactivation effect of different solutions is shown in Figure 4. The adsorption activity of sponge iron without reactivation was 33.8% of that before adsorption, and the adsorption capacity of phosphorus was significantly lower than that of sponge iron. Compared with hydrochloric acid, sulfuric acid has a better activation effect. When the sponge iron was modified with 6% H_2SO_4, the reuse efficiency was 98.2%, and

the adsorption capacity of the sponge iron to phosphorus was clearly restored. The main component of sponge iron is zero valent iron, so they have similar phosphorus removal mechanisms. The possible reactions are as follows:

1. The iron oxide on the surface of sponge iron dissociates or the iron ion is separated out by the corrosion of single iron, and the chemical reaction with phosphate produces insoluble salts, such as $FePO_4$, $Fe_3(PO_4)_2$, etc. After insoluble precipitates are formed, they easily cover the surface of sponge iron, which is not conducive to the further removal of phosphorus in the solution [41].
2. Iron ions generate long linear polynuclear hydroxyl complexes through hydrolysis and polymerization, and coordinate exchange with phosphates.
3. Under acidic and weakly alkaline conditions, sponge iron will combine with protons with positive charge; thus, electrostatic adsorption with negatively charged phosphate ions will occur [39].
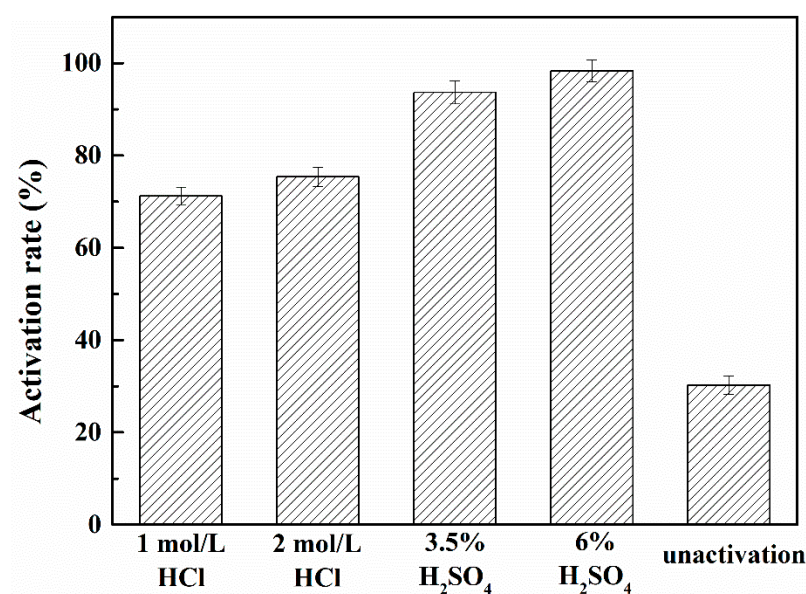

Figure 4. Effect of different solutions on the reactivation ability of sponge iron after desorption.

In the process of phosphorus removal by zero-valent iron the valence state of phosphorus does not change generally, and it mainly exists in the form of phosphate. There are complex interface processes in different redox environments. If $FePO_4$ and $Fe_3(PO_4)_2$ are the main components of phosphorus on the surface of sponge iron, it can be desorbed by acid. However, it was found that the desorption rate of phosphorus adsorbed by sulfuric acid on the surface of sponge iron was very low (less than 1%), so it was concluded that the phosphorus adsorbed by sponge iron was not mainly $FePO_4$ and $Fe_3(PO_4)_2$. On the contrary, when the NaOH solution is used for desorption, the desorption rate is as high as 95.5%. OH^- can destroy the state wherein the coordination body on the surface of the sponge iron combines with phosphate, and compete with the phosphate bonded on the surface of the sponge iron for the adsorption site, so that the phosphate can be desorbed. It can be concluded that the main mechanism of phosphorus removal in this study is the combination of phosphate and the hydroxyl complex on the surface of sponge iron through coordination exchange.

3.3. Effect of Sponge Iron Filtration Column on Phosphorus Removal

A continuous flow experiment was carried out to investigate the dynamic phosphorus removal characteristics of sponge iron. The relationship between phosphorus removal rate and operation time is shown in Figure 5.
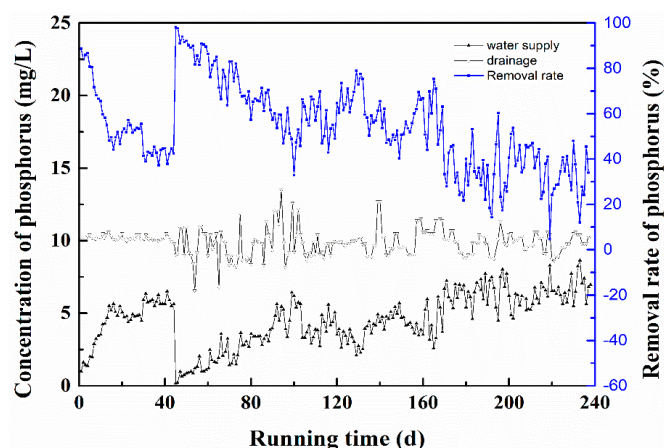
Figure 5. Continuous operation of phosphorus removal by sponge iron infiltration column.

The whole operation was divided into two stages: the initial operation stage and post-regeneration operation stage. In the initial stage of the operation, the phosphorus removal rate of the sponge iron percolation bed could reach 90%. With the increase in time, the removal rate of phosphorus began to decline. When running to the 18th day, the phosphorus removal rate was stable to around 50%. On the 43rd day, NaOH and H_2SO_4 were used to desorb phosphorus in situ and reactivate the sponge iron. After regeneration, the phosphorus removal ability of the system was restored, and the initial phosphorus removal rate could reach more than 90%. With the passage of time, the phosphorus removal rate decreased gradually. When running for 100 days, the phosphorus removal rate decreased to approximately 60%. Compared with that before regeneration, the phosphorus removal rate decreased slowly, indicating that the phosphorus removal performance of the sponge iron filter bed after regeneration was improved. A possible reason is that there were more active sites on the surface of the sponge iron due to the desorption of alkali and activation of acid. When it was operated to 240 days, the percolation bed did not show complete penetration, and the phosphorus removal rate eventually decreased to around 30%. In the whole operation stage, the volume load of the percolation bed was $120 \, g/dm^{-3}$, and the comprehensive phosphorus removal rate was 30–90%. After regeneration, the cumulative adsorption capacity of modified sponge iron reached 43,709 mg, and the adsorption capacity per unit volume reached $6.95 \, kg/m^3$. The sponge iron filter bed shows excellent continuous phosphorus removal ability and can effectively recover the phosphorus concentration. In situ regeneration can effectively restore the phosphorus removal performance of the filter bed [35,38].

3.4. Recovery of Phosphorus from Regenerated Waste Liquid by Struvite Precipitation

3.4.1. Effect of pH on the Recovery of Phosphorus

The above results show that sponge iron has good phosphorus adsorption and enrichment properties. In order to recycle the phosphorus after desorption, the method of producing struvite from the phosphorus recovered from the regenerated waste liquid was studied. Firstly, the effects of pH, Mg^{2+}, PO_4^{3-} and NH_4^+ molar ratio on the phosphorus recovery of the regenerated waste liquid were investigated. The main reaction equation for the formation of struvite is as follows:

$$Mg^{2+} + NH_4^+ + PO_4^{3-} + 6H_2O \rightarrow MgNH_4PO_4 \cdot 6H_2O \downarrow \tag{8}$$
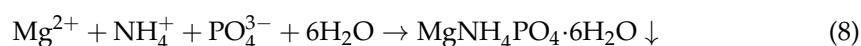
According to the principle of the chemical reaction, when the concentration product of Mg^{2+}, PO_4^{3-} and NH_4^+ is more than the solubility product constant of $MgNH_4PO_4 \cdot 6H_2O$, the struvite crystal precipitate will be formed. Although pH will not directly affect the ion activity product balance of struvite, it will affect the existing form and activity of the various ions that make up struvite when they reach equilibrium in water. When the phosphorus

content of the regenerated waste liquid is 826 mg/L, n (Mg^{2+}):n (PO_4^{3-}):n (NH^{4+}) = 1:1:1, the phosphorus recovery rate of the regenerated waste liquid at different pH is as shown in Figure 6a.
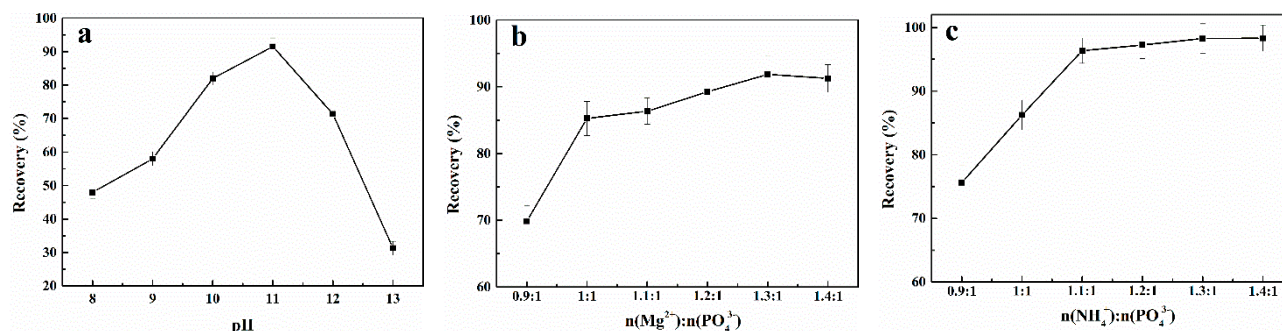

Figure 6. Effect of pH (**a**), Mg^{2+} concentration (**b**) and NH_4^+ concentration (**c**) on the recovery of phosphorus.

Figure 6a shows the effect of the initial pH on the recovery of struvite in the regenerated waste liquid. It was found that when the pH of the system was less than 8, almost no precipitates were produced. With the increase in pH, a white precipitate appeared and the recovery of phosphorus increased. Although the recovery rate of phosphorus in the solution reaches the maximum at pH = 11, which is 93.2%, it is found that there is a latex-like substance in the sediment, which is quite different from that at pH = 9–10. An explanation may be the by-product outside the guano stone, which is also verified in the following product analysis [35,38]. The theoretical calculation shows that when the pH is 10–11, ammonia will dissociate from $MgNH_4PO_4$ and form more insoluble $Mg_3(PO_4)_2$ [30]. When the pH is more than 11, there will be $Mg(OH)_2$. When the pH is more than 12, there is obvious ammonia gas escaping from the solution, and the utilization rate of ammonia nitrogen decreases, which is not conducive to the formation of struvite. When pH = 10, the amount of acid added is lower, and the ratio of phosphorus recovery to guano stone is the highest, which is the best pH for guano stone recovery.

3.4.2. Effect of Magnesium Salt Dosage

The theoretical molar ratio of Mg^{2+}, PO_4^{3-} and NH_4^+ for the formation of struvite is 1:1:1, but the composition of the regenerated waste liquid is relatively complex, as it contains elements such as iron, calcium, carbon and silicon. Mg^{2+}, PO_4^{3-} may generate other precipitates in the reaction. Therefore, it is necessary to increase the content of some ions, promote the balance to move forward, and improve the phosphorus recovery. Control pH = 10, n (PO_4^{3-}):n (NH_4^+) = 1:1, a change in Mg^{2+} dosage, and the effect of dosage on phosphorus recovery are shown in Figure 6b. With the increase in Mg^{2+} concentration, the recovery of phosphorus also increased. When the ratio of n (Mg^{2+}):n (PO_4^{3-}) increased from 0.9 to 1.3, the recovery of phosphorus increased from 69.4% to 93.4%, indicating that the reaction of struvite formation was incomplete when the ratio of n (Mg^{2+}):n (PO_4^{3-}) < 1.3. After this, the dosage of Mg^{2+} was increased to 1.4:1, and the phosphorus recovery rate did not increase significantly, indicating that, at this time, Mg^{2+} was excessive and reacted with other ions to form non-struvite precipitation. Therefore, the optimum ratio of n (Mg^{2+}):n (PO_4^{3-}) is 1.3:1.

3.4.3. Effect of Ammonia Nitrogen Dosage

We controlled the magnesium salt dosage ratio of n (Mg^{2+}):n (PO_4^{3-}) to 1.3:1, pH = 10, and investigated the effect of ammonia nitrogen dosage on phosphorus recovery (Figure 6c). The results showed that the phosphorus recovery increased with the increase in ammonia nitrogen. When the ratio of n (NH_4^+):n (PO_4^{3-}) increased from 0.9 to 1.1, the phosphorus recovery increased from 76.3% to 96.3%. With the increase in ammonia and

nitrogen, phosphorus recovery was not significantly improved. From the perspective of environmental protection and economic interests, the best ratio of n (NH_4^+):n (PO_4^{3-}) is 1.1:1. In order to achieve the best recovery of phosphorus, these three ions must be added to the solution in an appropriate proportion [9,25].

3.4.4. System Experiment

On the basis of the above research, in order to test the reliability of the best process conditions, several groups of overall tests were carried out. The results are shown in Figure 7. When the ratio of n $(Mg^{2+}$:n (PO_4^{3-}):n (NH_4^+) was increased from 1:1:1 to 1.3:1:1.1, the recovery of phosphorus clearly increased. When the ratio was increased to 1.4:1:1.2, the recovery of phosphorus was not significantly increased. pH is the main factor that restricts the recovery of phosphorus. The optimal process conditions are: pH = 10, n (NH_4^+):n (PO_4^{3-}) = 1.1, n (Mg^{2+}):n (PO_4^{3-}) = 1.3.
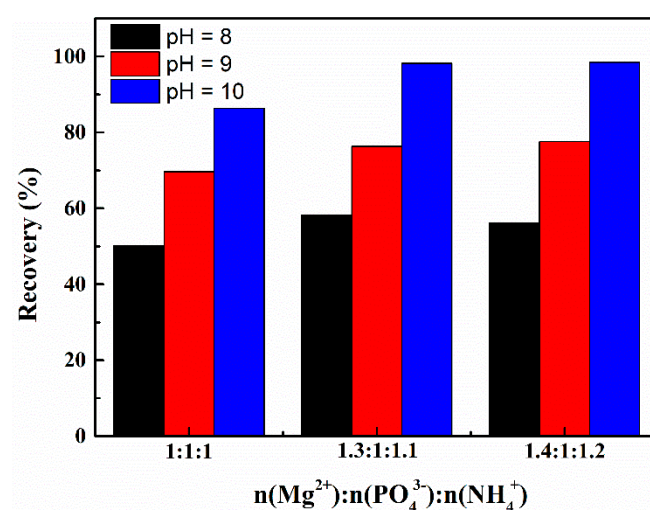

Figure 7. Results of optimization experiment.

3.4.5. XRD Analysis of Precipitation Products

Under the optimum molar ratio, the XRD diffraction patterns of the test products with pH = 9, 10 and 11 were analyzed. The results are shown in Figure 8.
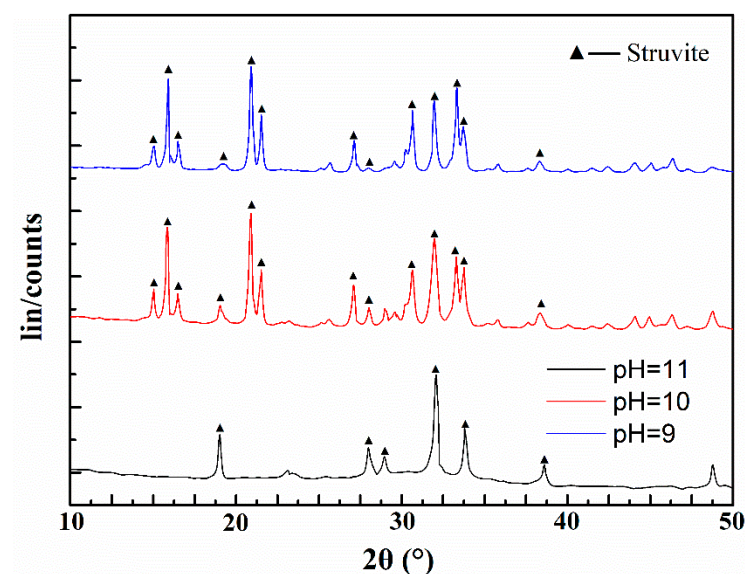

Figure 8. XRD patterns of phosphorus products under different pH.

It can be seen that when the pH is 9, the peak type of the X-ray diffraction pattern of the precipitate is basically consistent with the standard pattern of $MgNH_4PO_4 \cdot 6H_2O$, and no other crystal image is shown, indicating that the main component of the precipitate is struvite, and the purity of the precipitate is high. However, the amount of precipitation products is very small and the phosphorus recovery rate is obviously low. When the pH is 10, the diffraction peak position is almost the same, but the intensity is obviously enhanced, indicating that most of the products are guano stone. Compared with the spectrum at pH 9, some impurity peaks are doped, which indicates that a few by-products are doped, but the amount of precipitated products is significantly higher than the product quality at pH 9, which is also consistent with the high phosphorus recovery rate of pH = 10 observed in the test process, the obvious stratification limit, and the better sedimentation performance. When the pH is 11, there is no obvious crystal characteristic peak of the precipitate, which is completely inconsistent with the diffraction peak of the $MgNH_4PO_4 \cdot 6H_2O$ standard spectrum, indicating that the product may not be struvite.

4. Conclusions

1. Using 6% sulfuric acid to modify sponge iron could improve the adsorption capacity of phosphorus, and in this experiment the theoretical maximum adsorption capacity of modified sponge iron was increased by 335% compared with that before modification. When the modified sponge iron was saturated with phosphorus, its phosphorus removal ability could be restored by desorption and reactivation, and the activation rate could reach 98.2%.
2. The sponge iron percolation bed had a good dynamic phosphorus removal performance, and the accumulated phosphorus adsorption capacity reached 6.95 kg/m^3. The carrier was easy to activate and regenerate, and thus it could be used to effectively recover phosphorus from water containing phosphorus.
3. pH is the main factor affecting the production of struvite from alkali regeneration waste liquid. The optimal conditions for the preparation of struvite from phosphorus containing desorption solution achieved by adjusting the pH and adding nitrogen and magnesium are: initial pH = 10, n (Mg^{2+}):n (PO_4^{3-}):n (NH_4^+) = 1.3:1:1.1. Under the optimal conditions, the phosphorus recovery rate could reach 97.8%.

Author Contributions: P.C. and B.W. conceived and designed the experiments; X.W. and W.X. prepared the samples and performed the experiments; P.C. and X.W. analyzed the data and B.W. contributed to the writing and revision of the paper. All authors have read and agreed to the published version of the manuscript.

Conflicts of Interest: The authors declare no conflict of interest.

References

1. Xiao, W.; Ke, S.; Quan, N.; Zhou, L.; Wang, J.; Zhang, L.; Dong, Y.; Qin, W.; Qiu, G.; Hu, J. The Role of Nanobubbles in the Precipitation and Recovery of Organic-Phosphine-Containing Beneficiation Wastewater. *Langmuir* **2018**, *34*, 6217–6224. [CrossRef]
2. Han, C.; Qin, Y.; Zheng, B.; Ma, Y.; Yang, C.; Liu, Z.; Zhuang, D.; Zhao, Y. Geochemistry of phosphorus release along transect of sediments from a tributary backwater zone in the Three Gorges Reservoir. *Sci. Total Environ.* **2020**, *722*, 136964. [CrossRef]
3. Xu, R.; Zhang, M.; Mortimer, R.J.G.; Pan, G. Enhanced Phosphorus Locking by Novel Lanthanum/Aluminum–Hydroxide Composite: Implications for Eutrophication Control. *Environ. Sci. Technol.* **2017**, *51*, 3418–3425. [CrossRef] [PubMed]
4. Zhang, B.; Ding, W.; Xu, B.; Wang, L.; Li, Y.; Zhang, C. Spatial characteristics of total phosphorus loads from different sources in the Lancang River Basin. *Sci. Total Environ.* **2020**, *722*, 137863. [CrossRef]
5. Yogev, U.; Vogler, M.; Nir, O.; Londong, J.; Gross, A. Phosphorous recovery from a novel recirculating aquaculture system followed by its sustainable reuse as a fertilizer. *Sci. Total Environ.* **2020**, *722*, 137949. [CrossRef]
6. Blatter, M.; Furrer, C.; Cachelin, C.P.; Fischer, F. Phosphorus, chemical base and other renewables from wastewater with three 168-L microbial electrolysis cells and other unit operations. *Chem. Eng. J.* **2020**, *390*, 124502. [CrossRef]
7. Afridi, M.N.; Lee, W.-H.; Kim, J.-O. Application of synthesized bovine serum albumin-magnetic iron oxide for phosphate recovery. *J. Ind. Eng. Chem.* **2020**, *86*, 113–122. [CrossRef]

8. Gao, Y.; Fang, Z.; Chen, C.; Zhu, X.; Liang, P.; Qiu, Y.; Zhang, X.; Huang, X. Evaluating the performance of inorganic draw solution concentrations in an anaerobic forward osmosis membrane bioreactor for real municipal sewage treatment. *Bioresour. Technol.* **2020**, *307*, 123254. [CrossRef]

9. Chi Thanh, V.; Wu, T. Magnetic porous NiLa-Layered double oxides (LDOs) with improved phosphate adsorption and antibacterial activity for treatment of secondary effluent. *Water Res.* **2020**, *175*, 115679.

10. Kress, N.; Gertner, Y.; Shoham-Frider, E. Seawater quality at the brine discharge site from two mega size seawater reverse osmosis desalination plants in Israel (Eastern Mediterranean). *Water Res.* **2019**, *171*, 115402. [CrossRef]

11. Chen, Y.; Lin, H.; Yan, W.; Huang, J.; Wang, G.; Shen, N. Alkaline fermentation promotes organics and phosphorus recovery from polyaluminum chloride-enhanced primary sedimentation sludge. *Bioresour. Technol.* **2019**, *294*, 122160. [CrossRef] [PubMed]

12. Yang, H.; Liu, J.; Hu, P.; Zou, L.; Li, Y.-Y. Carbon source and phosphorus recovery from iron-enhanced primary sludge via anaerobic fermentation and sulfate reduction: Performance and future application. *Bioresour. Technol.* **2019**, *294*, 122174. [CrossRef]

13. Kabenge, I.; Ouma, G.; Aboagye, D.; Banadda, N. Performance of a constructed wetland as an upstream intervention for stormwater runoff quality management. *Environ. Sci. Pollut. Res.* **2018**, *25*, 36765–36774. [CrossRef]

14. Tong, Y.R.; McNamara, P.J.; Mayer, B.K. Fate and impacts of triclosan, sulfamethoxazole, and 17 beta-estradiol during nutrient recovery via ion exchange and struvite precipitation. *Environ. Sci. Water Res. Technol.* **2017**, *3*, 1109–1119. [CrossRef]

15. Koh, K.Y.; Zhang, S.; Chen, J.P. Improvement of Ultrafiltration for Treatment of Phosphorus-Containing Water by a Lanthanum-Modified Aminated Polyacrylonitrile Membrane. *ACS Omega* **2020**, *5*, 7170–7181. [CrossRef]

16. Huang, X.; Zhu, T.; Duan, W.; Liang, S.; Li, G.; Xiao, W. Comparative studies on catalytic mechanisms for natural chalcopyrite-induced Fenton oxidation: Effect of chalcopyrite type. *J. Hazard. Mater.* **2019**, *381*, 120998. [CrossRef]

17. Muisa, N.; Nhapi, I.; Ruziwa, W.; Manyuchi, M.M. Utilization of alum sludge as adsorbent for phosphorus removal in municipal wastewater: A review. *J. Water Process Eng.* **2020**, *35*, 101187. [CrossRef]

18. Karami, M.; Koohestani, H.; Gholami, H. Investigation of the effect of geometrical shape of sponge iron on the operating parameters of the induction furnace. *Can. Met. Q.* **2022**, 1–6. [CrossRef]

19. Xiao, W.; Zhao, Y.; Yang, J.; Ren, Y.; Yang, W.; Huang, X.; Zhang, L. Effect of Sodium Oleate on the Adsorption Morphology and Mechanism of Nanobubbles on the Mica Surface. *Langmuir* **2019**, *35*, 9239–9245. [CrossRef] [PubMed]

20. Lin, J.; He, S.; Wang, X.; Zhang, H.; Zhan, Y. Removal of phosphate from aqueous solution by a novel $Mg(OH)_2/ZrO_2$ composite: Adsorption behavior and mechanism. *Colloids Surf. Physicochem. Eng. Asp.* **2019**, *561*, 301–314. [CrossRef]

21. Xiao, W.; Ren, Y.-X.; Yang, J.; Cao, P.; Wang, J.; Qin, W.-Q.; Qiu, G.-Z. Adsorption mechanism of sodium oleate and styryl phosphonic acid on rutile and amphibole surfaces. *Trans. Nonferr. Met. Soc. China* **2019**, *29*, 1939–1947. [CrossRef]

22. Yuan, L.; Qiu, Z.; Yang, J.; Li, Z.; Farooq, U.; Lu, Y.; Lyu, S. Adsorption performance and mechanism for phosphate removal by cerium hydroxide loaded on molecular sieve. *J. Taiwan Inst. Chem. Eng.* **2018**, *93*, 450–460. [CrossRef]

23. Zhang, J.; Ding, W.; Zhang, Z.; Xu, J.; Wen, Y. Preparation of black phosphorus-PEDOT:PSS hybrid semiconductor composites with good film-forming properties and environmental stability in water containing oxygen. *RSC Adv.* **2016**, *6*, 76174–76182. [CrossRef]

24. Hadroug, S.; Jellali, S.; Azzaz, A.A.; Kwapinska, M.; Hamdi, H.; Leahy, J.J.; Jeguirim, M.; Kwapinski, W. Valorization of salt post-modified poultry manure biochars for phosphorus recovery from aqueous solutions: Investigations on adsorption properties and involved mechanism. *Biomass Convers. Biorefin.* **2021**, 1–16. [CrossRef]

25. Pellicer-Castell, E.; Belenguer-Sapiña, C.; Amorós, P.; El Haskouri, J.; Herrero-Martínez, J.M.; Mauri-Aucejo, A. Study of silica-structured materials as sorbents for organophosphorus pesticides determination in environmental water samples. *Talanta* **2018**, *189*, 560–567. [CrossRef]

26. Gong, W.; Fan, Y.; Xie, B.; Tang, X.; Guo, T.; Luo, L.; Liang, H. Immobilizing Microcystis aeruginosa and powdered activated carbon for the anaerobic digestate effluent treatment. *Chemosphere* **2019**, *244*, 125420. [CrossRef]

27. Ebrahiminejad, M.; Karimzadeh, R. Influence of phosphorus content on properties and performance of NiW nanocatalyst supported on activated red mud in atmospheric diesel hydrodesulfurization. *J. Hazard. Mater.* **2019**, *384*, 121485. [CrossRef] [PubMed]

28. Zhan, Y.; Wu, X.; Lin, J. Combined use of calcium nitrate, zeolite, and anion exchange resin for controlling phosphorus and nitrogen release from sediment and for overcoming disadvantage of calcium nitrate addition technology. *Environ. Sci. Pollut. Res.* **2020**, *27*, 24863–24878. [CrossRef]

29. Wu, B.; Fang, L.; Fortner, J.D.; Guan, X.; Lo, I.M. Highly efficient and selective phosphate removal from wastewater by magnetically recoverable $La(OH)_3/Fe_3O_4$ nanocomposites. *Water Res.* **2017**, *126*, 179–188. [CrossRef] [PubMed]

30. Jellali, S.; Khiari, B.; Usman, M.; Hamdi, H.; Charabi, Y.; Jeguirim, M. Sludge-derived biochars: A review on the influence of synthesis conditions on pollutants removal efficiency from wastewaters. *Renew. Sustain. Energy Rev.* **2021**, *144*, 111068. [CrossRef]

31. Sun, H.; Zhou, Q.; Zhao, L.; Wu, W. Enhanced simultaneous removal of nitrate and phosphate using novel solid carbon source/zero-valent iron composite. *J. Clean. Prod.* **2021**, *289*, 125757. [CrossRef]

32. Ma, J.; Ren, S.; Song, Y.; Wang, D.; Men, B.; Zhao, H. Advances in the Application of Zero-Valent Iron Technology in the Field of Wastewater Treatment. *Chemistry* **2019**, *82*, 3–11.

33. Sleiman, N.; Deluchat, V.; Wazne, M.; Mallet, M.; Courtin-Nomade, A.; Kazpard, V.; Baudu, M. Phosphate removal from aqueous solution using ZVI/sand bed reactor: Behavior and mechanism. *Water Res.* **2016**, *99*, 56–65. [CrossRef]

34. Wang, Y.; Feng, Y.; Jiang, J.; Yao, J. Designing of Recyclable Attapulgite for Wastewater Treatments: A Review. *ACS Sustain. Chem. Eng.* **2018**, *7*, 1855–1869. [CrossRef]

35. Easun, T.L.; Moreau, F.; Yan, Y.; Yang, S.; Schröder, M. Structural and dynamic studies of substrate binding in porous metal–organic frameworks. *Chem. Soc. Rev.* **2016**, *46*, 239–274. [CrossRef]

36. Xue, R.; Xu, J.; Gu, L.; Pan, L.; He, Q. Study of Phosphorus Removal by Using Sponge Iron Adsorption. *Water Air Soil Pollut.* **2018**, *229*, 161. [CrossRef]

37. Wang, G.-B.; Wang, Y.; Zhang, Y. Combination effect of sponge iron and calcium nitrate on severely eutrophic urban landscape water: An integrated study from laboratory to fields. *Environ. Sci. Pollut. Res.* **2018**, *25*, 8350–8363. [CrossRef]

38. Strauch, S.M.; Wenzel, L.C.; Bischoff, A.; Dellwig, O.; Klein, J.; Schüch, A.; Wasenitz, B.; Palm, H.W. Commercial African Catfish (Clarias gariepinus) Recirculating Aquaculture Systems: Assessment of Element and Energy Pathways with Special Focus on the Phosphorus Cycle. *Sustainability* **2018**, *10*, 1805. [CrossRef]

39. Wang, Y.; Li, J.; Zhai, S.; Wei, Z.; Feng, J. Enhanced phosphorus removal by microbial-collaborating sponge iron. *Water Sci. Technol.* **2015**, *72*, 1257–1265. [CrossRef] [PubMed]

40. Jiang, C.; Jia, L.; He, Y.; Zhang, B.; Kirumba, G.; Xie, J. Adsorptive removal of phosphorus from aqueous solution using sponge iron and zeolite. *J. Colloid Interface Sci.* **2013**, *402*, 246–252. [CrossRef]

41. Park, I.; Higuchi, K.; Tabelin, C.B.; Jeon, S.; Ito, M.; Hiroyoshi, N. Suppression of arsenopyrite oxidation by microencapsulation using ferric-catecholate complexes and phosphate. *Chemosphere* **2021**, *269*, 129413. [CrossRef] [PubMed]